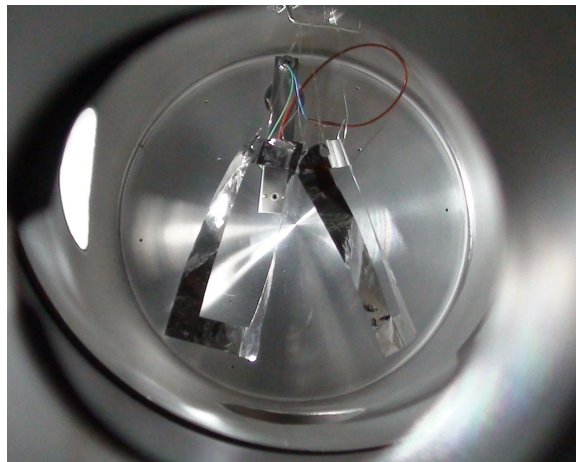


NASA Langley Supported Study
Electrostatic Charge Deflection Experiments
Final Report



Principal Investigator:

Hanspeter Schaub¹
University of Colorado, Boulder, CO 80309-0431

October 10, 2011

¹Associate Professor, H. Joseph Smead Fellow, hanspeter.schaub@colorado.edu, (303) 492-2767

Abstract

This report describes the research completed during a 3-month study at the University of Colorado on charge deflection using electrostatically inflated membrane structures (EIMS). The research is motivated by the desire to achieve active space radiation shielding using large lightweight gossamer space structures. The goal is to investigate if a charged Gossamer structure can perform charge deflections without significant structural instabilities occurring. In this study, experiments are performed with up to 5kV of charging, and an electron flux source with up to 5keV of energy. While these charge flux energy levels are much less than those encountered in space, the fundamental coupled interaction of charged Gossamer structures with the ambient charge flux can be experimentally investigated. Of interest are, will the EIMS remain inflated during the charge deflections, and are there visible charge flux interactions. Aluminum coated mylar membrane prototype structures are created to test their inflation capability using electrostatic charging. To simulate the charge flux, a 5keV electron emitter is assembled. The remaining charge flux at the end of the test chamber is measured with a Faraday cup mounted on a movable boom. A range of experiments with this electron emitter and detector were performed within a 30×60cm vacuum chamber. First, experiments are performed to illustrate that the electrostatic potentials are sufficient to inflate EIMS in this strong vacuum environment of 10^{-7} Torr. Next, experiments are performed with the charge flux aimed at the EIMS in both charged and uncharged configurations. The amount of charge shielding by EIMS was studied for different combinations of membrane structure voltages and electron energies. The pattern of charge distribution around the structure was also studied as well as the stability of the structures in the charge flow. Depending on the EIMS potential levels, the amounts of charge flux reductions were measured to be around 80-99%. The electron energies are not sufficient to punch through the membrane layers. However, the charge flux interactions with the vacuum chamber boundaries result in a small, but noticeable ambient charge flux even behind the structure. The exact cause of this flux, and methods to reduce this, will be studied in future work. The charge deflection experiments illustrate that the EIMS remain inflated during charge deflection, but will experience small amplitude oscillations. The stronger the EIMS potential, the stiffer the structural response was. The exact cause of this oscillation is to be investigated in future work.

Table of Contents

1	Introduction	1
1.1	EIMS Background	2
1.2	Radiation Shielding Background	3
1.3	Project Scope and Budget	4
1.4	Research Team	5
2	Experimental Setup	6
2.1	High Voltage EIMS Charging Setup	6
2.2	Charge Deflection Hardware Components	7
2.3	Experimental Structures	9
3	Experiments and Results	11
3.1	Atmospheric Inflation Experiments	11
3.2	Vacuum Inflation Experiments	12
3.3	Charge Deflection Experiments	14
3.3.1	Shielding Experiments	15
3.3.2	Charge Deflection Pattern	16
3.3.3	Stability in an Electron Flow	18
4	Conclusions and Future Work	21
4.1	Study Conclusions	21
4.2	Future Work Considerations	21

Chapter 1

Introduction

Radiation shielding is an important design criteria for any space mission, especially those involving human space explorers. A long-term goal for NASA is to use lightweight structures for active radiation shielding to create safe habitation zones. An example of this is charged membrane structures deflecting the harmful radiation ion-flux as seen in Figure 1.1. This report describes an investigation into the use of electrostatic fields for radiation shielding through such charged membrane structures. The membrane structures consist of layers of conducting material which self-repel to inflate when an absolute charge is applied. The electrostatically inflated membrane structure (EIMS) is envisioned as a lightweight structure which can act as shield to charged particles.

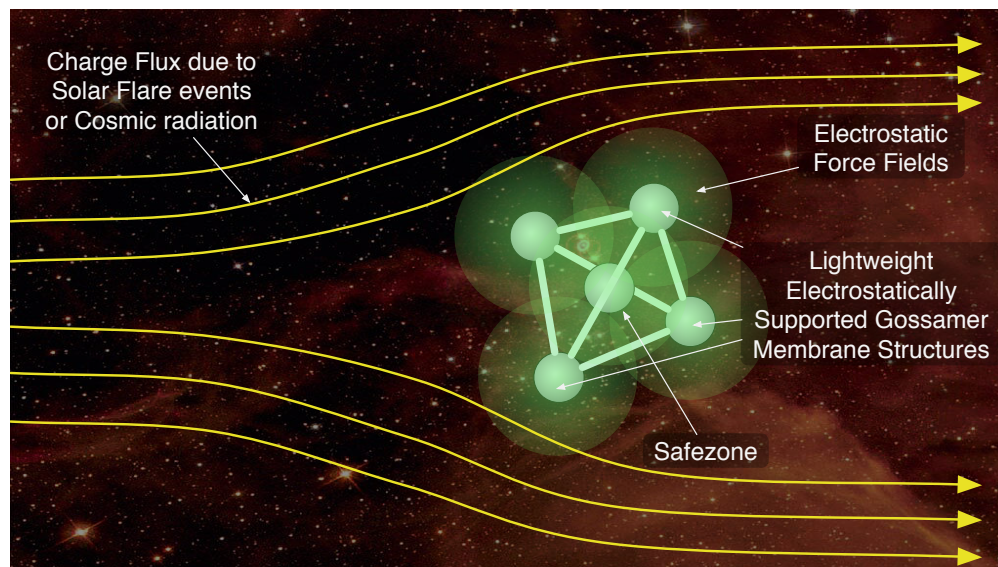


Figure 1.1: Concept illustration of radiation shielding with an electrostatically charged structure

An experimental setup was designed to study the use of EIMS for charge deflection. An electron source and detector were mounted on opposite sides of an EIMS in a vacuum chamber. Experiments were performed to study the radiation shielding capabilities, the charge deflection pattern, and the stability of the structure. The report will discuss the hardware and software development for experiments, as well as the results of experiments in atmospheric conditions, a vacuum chamber, and a plasma environment.

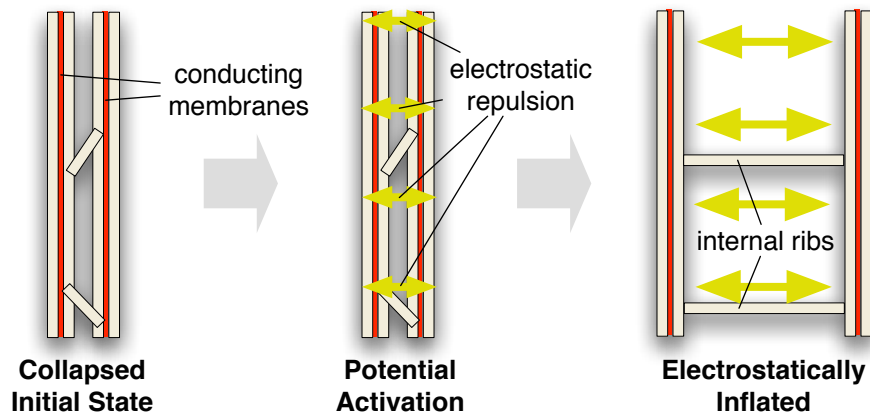


Figure 1.2: Illustration of electrostatic inflation of a membrane structure. The membrane interconnects (ribs) limit the amount of expansion and control the EIMS shape and thickness.

1.1 EIMS Background

Electrostatically Inflated Membrane Structures or EIMS employ layers of lightweight membrane with a conductive coating along with active charge control to create inflationary electrostatic forces as shown in Figure 1.2. With this concept, extremely large deployed to stored volume ratios are feasible. The stored membrane structure will be packaged very tightly and does not require any pressurized gas storage devices. Rather, active charge control in the form of charge emission is employed to control the absolute EIMS potential. With EIMS it is feasible that the deployed structures are open shapes. Punctures due to micro-meteorites will have a negligible impact as this concept does not suffer from leakage concerns like gas-inflated Gossamer structures.

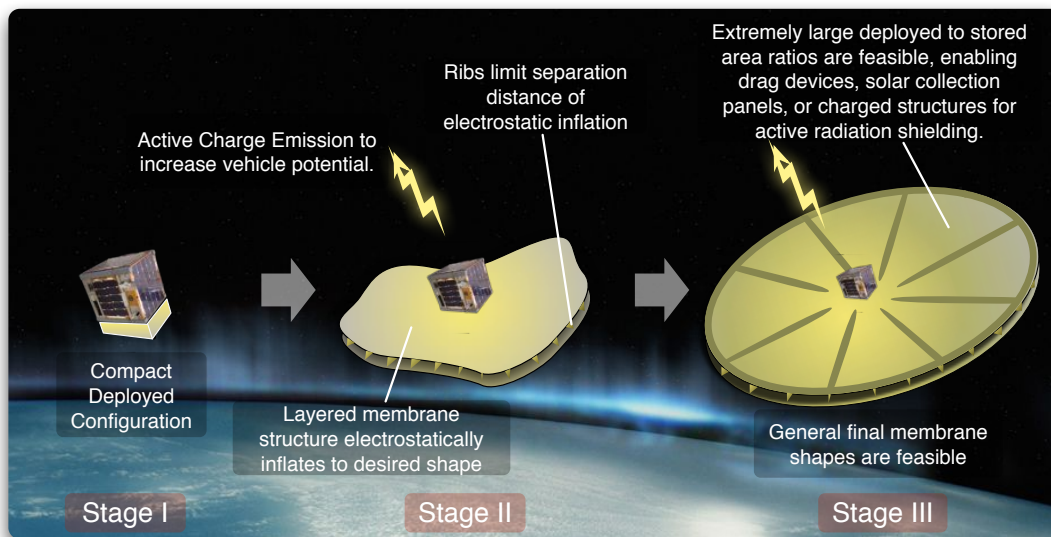


Figure 1.3: Electrostatic inflation concept illustration.

An illustration of the EIMS concept deploying on a small satellite is shown in Figure 1.3. This concept of electrostatic inflation of membrane space structures is explored in References 1 and

2. The analysis in these references includes determination of the voltage required on a two-membrane sandwich structure to offset normal compressive orbital perturbations to the structure. The compressive pressures would tend to collapse the membrane structure, thus must be compensated by the inflation pressure. In GEO, solar radiation pressure is the dominant compression pressure of the orbital perturbations. In LEO, solar radiation pressure dominates until an orbit altitude of approximately 500km, under which atmospheric drag becomes the dominant pressure. To offset the normal compressive orbital pressures, it was found that hundreds of volts are required in GEO and a few kilovolts in LEO. Figure 1.4 illustrates a box-like membrane structure overcoming 1-g of gravity to inflated using a few kilovolts in atmospheric laboratory conditions.



Figure 1.4: *Atmospheric Electrostatic Inflation Experiment of a Box-Like Membrane Structure*

Many challenges to the electrostatic inflation concept exist, such as plasma Debye shielding, space weather, orbital perturbations which may tend to collapse the structure, and complex structural dynamics. In Reference 1, plasma effects on EIMS were briefly discussed in relation to the Debye shielding phenomenon. In the space plasma environment, electrons and ions rearrange to maintain macroscopic neutrality when perturbed by an external electric field.³ This phenomena causes a steeper dropoff in the potential surrounding a charged object than would occur in a vacuum, thus limiting electrostatic force actuation, especially in cold, dense plasmas. In addition to Debye shielding, the plasma complicates charging of a spacecraft due to ram effects as a spacecraft moves through the plasma and also wake effects behind the moving craft. For the EIMS concept, it will be important to understand how the charge will flow around the structure and affect inflation. Experiments described within this report were aimed at studying shape stability during charge deflection experiments. Such tests require that the charging experiments are performed in a controlled vacuum chamber with high-quality pumps to avoid issues with ionization of a low-pressure atmosphere. For the experiments discussed in this report, the chamber achieved a vacuum of 10^{-7} Torr for inflation tests and 10^{-6} Torr for charge deflection experiments.

1.2 Radiation Shielding Background

Radiation shielding is a critical challenge with envisioned manned space exploration activities. The dangers of radiation to biological tissue must be well understood, and protection incorporated into any space travel concept. This is particularly true for long duration missions and travel beyond Low Earth Orbit. Radiation shielding can be accomplished with passive or active methods, or a combination of the two. Current designs employ passive damping where sufficient material is present to absorb enough of the harmful high-energy ion radiation. This concept has the benefit that no active control is required, and thus it provides a robust solution. One drawback of passive shielding is the mass of the materials required for adequate radiation safety. This mass is a challenge when designing interplanetary human explorations. A savings in the mass required to

perform radiation shielding would enable significant mission cost reductions.

Use of electrostatic fields is one active method which provides an alternative to bulk material passive shielding.⁴ Other forms of active shielding include plasma shields, confined magnetic fields, and unconfined magnetic fields.⁵ Some of the challenges of active electrostatic shielding, such as high potentials and size limitations due to electrical breakdown, have deterred further research on the subject.⁶ In Reference 6, Tripathi challenges the claim that electrostatic shielding may be unsuitable and explores a feasible design for radiation shielding, as shown in Figure 1.5.

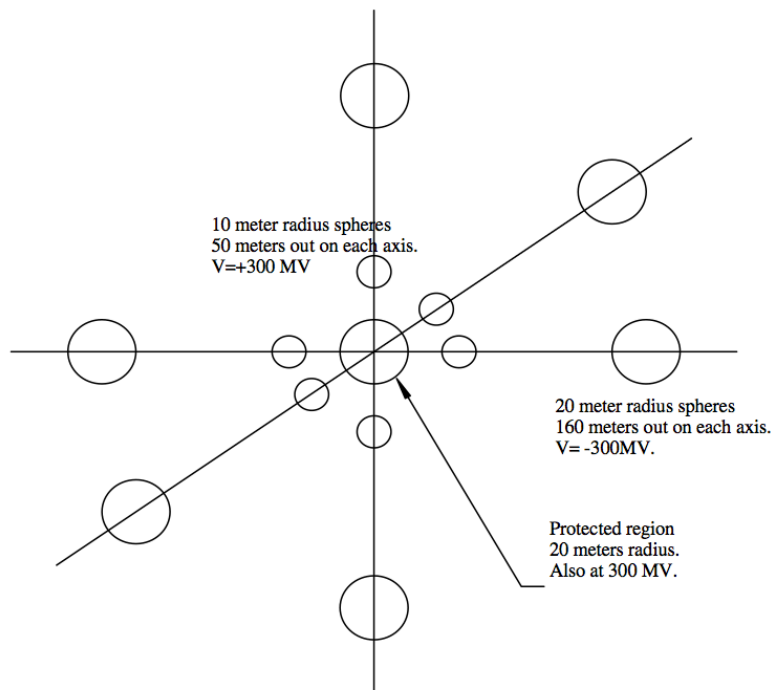


Figure 1.5: *Electrostatic space radiation shielding concept*⁶

The 10-sphere design requires potentials of 300 Megavolts, and would be used in conjunction with passive material shielding. The author notes that the ability to achieve 300 MV potential levels remains as future work. For EIMS applications, only potentials in the tens of kilovolts have been explored to study the ability to inflate and overcome membrane residual stresses, therefore investigating the feasibility of potentials beyond tens of kilovolts is part of future work. Radiation shielding capabilities of EIMS charged within a range of 0-5 kV are described in the results section of this report.

1.3 Project Scope and Budget

The electrostatic charge deflection experiments were part of a 3-month study conducted at the University of Colorado at Boulder from June to August, 2011. The CU facilities used for the study include a small vacuum chamber that is 30cm in diameter and 60cm long with pressures feasible to the 10^{-7} Torr range. Such a chamber was ideal for cost-effective initial deployment and shape testing of EIMS test concepts. This vacuum chamber, pumps, and high-voltage interfaces are owned by Dr. Sternovsky of the University of Colorado. He is an international expert on

dusty plasma physics and high-voltage charge transfer experiments. He provided guidance on the experimental setup, and his researchers helped Dr. Schaub's students learn how to use their facility. Without their help and knowledge on performing vacuum chamber charging experiments the 3-month project would not have been possible.

The total budget for the summer project was \$20,923. These funds were used to cover PI support, research assistant support, and laboratory materials and equipment. Key equipment which was purchased includes a high voltage power supply, data-acquisition hardware, and a Faraday cup charge sensor.

1.4 Research Team

The research for the 3-month study was led Dr. Schaub's Ph.D. graduate student Laura Stiles. She led the preliminary atmospheric EIMS inflation experiments, as well as the vacuum chamber test development and analysis. Another Ph.D. student, Carl Seubert, provided support in setting up the data acquisition recording software. This code also provides manual and computer controlled voltage control of the electrostatic power supply charging the EIMS structure. Project direction and advising were provided by Dr. Hanspeter Schaub with collaboration and support by Dr. Zoltan Sternovsky of the University of Colorado. Two undergraduate students provided technical assistance with experiments. Nicolas Zinner led the design of the data acquisition system and aided in the setup of the vacuum chamber experiments. Jack Mills aided in membrane structure construction and running experiments within the chamber.

Chapter 2

Experimental Setup

The setup for the radiation experiments includes an electron gun at one end of a vacuum chamber and a Faraday cup positioned behind a membrane structure at the opposite end of the chamber. The electron gun emits electrons and the Faraday cup measures the current, allowing observation of the flow of electrons around an EIMS structure and providing insight into how an EIMS structure can be used for radiation shielding. The EIMS structure is charged with a high voltage power supply system external to the vacuum chamber. The concept is illustrated in Figure 2.1.

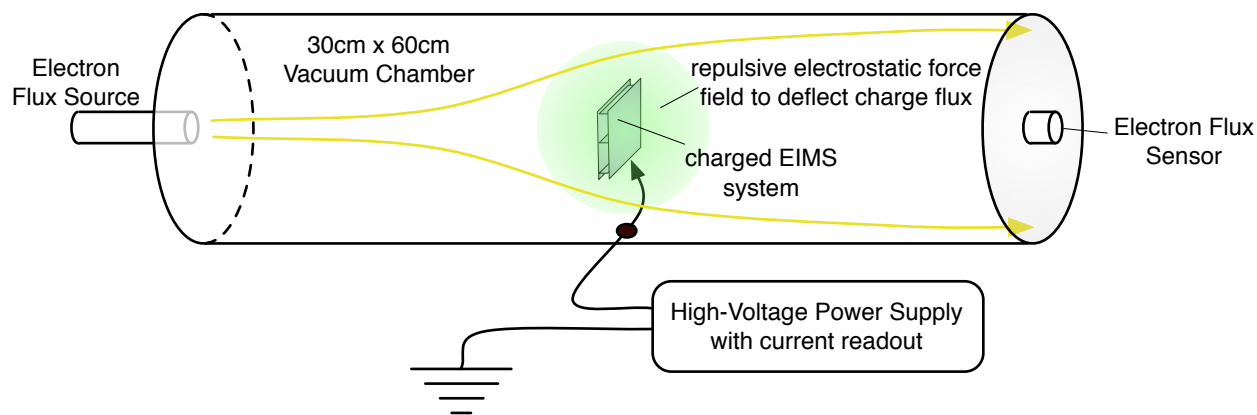


Figure 2.1: Concept illustration for the radiation shielding experimental setup

2.1 High Voltage EIMS Charging Setup

The first component of the experimental hardware which was designed and built was a high voltage EIMS charging setup. The charging setup is used to apply a desired voltage to the membrane structures for inflation.

Figure 2.2 displays a diagram of the setup. The high voltage is supplied by an Ultravolt 40A Series high voltage DC-DC converter. This device supplies up to -40kV to the membrane structures. The voltage magnitude is controlled by a user through a Graphical User Interface on a Macbook computer, as shown in Figure 2.3. A National Instruments USB-6008 data acquisition device is used to drive the power supply and also to record current and voltage data.

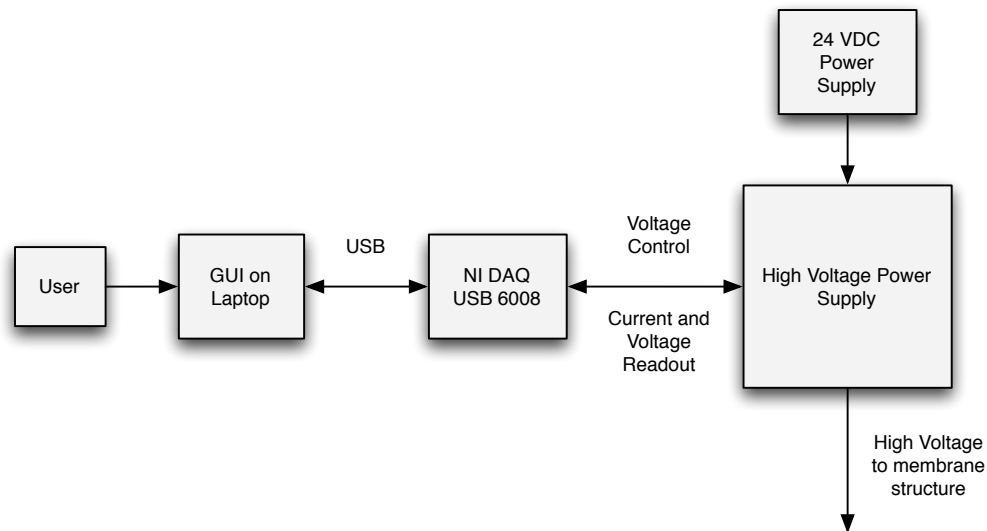


Figure 2.2: Block diagram of high voltage charging setup for membrane structures

This custom software allows the EIMS to be charged to a particular absolute voltage by either manually moving the voltage slider, or by running a predefined voltage history on the structure. For the following experiments, the setup is such that the voltage is being held at a fixed value while charge flux and EIMS stability observations are made.

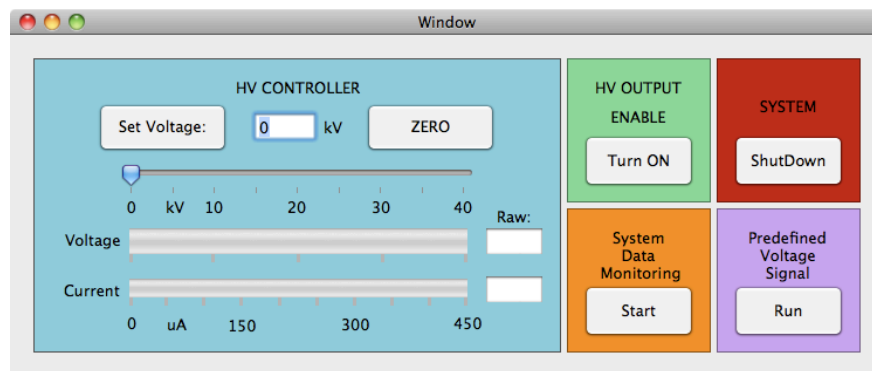


Figure 2.3: Graphical User Interface for operating the high voltage charging setup

2.2 Charge Deflection Hardware Components

Figure 2.4 illustrates each of the components of the experimental setup. A summary of the setup is as follows: the electron gun is heated and electrons produced by thermionic emission are accelerated from the filament, biased to -5 kV, toward the grid, which is grounded. A membrane structure hangs between the electron gun and a detector to read the current behind and around the structure.

Figure 2.5 shows the constructed electron emitter. The filament is heated and electrons accel-

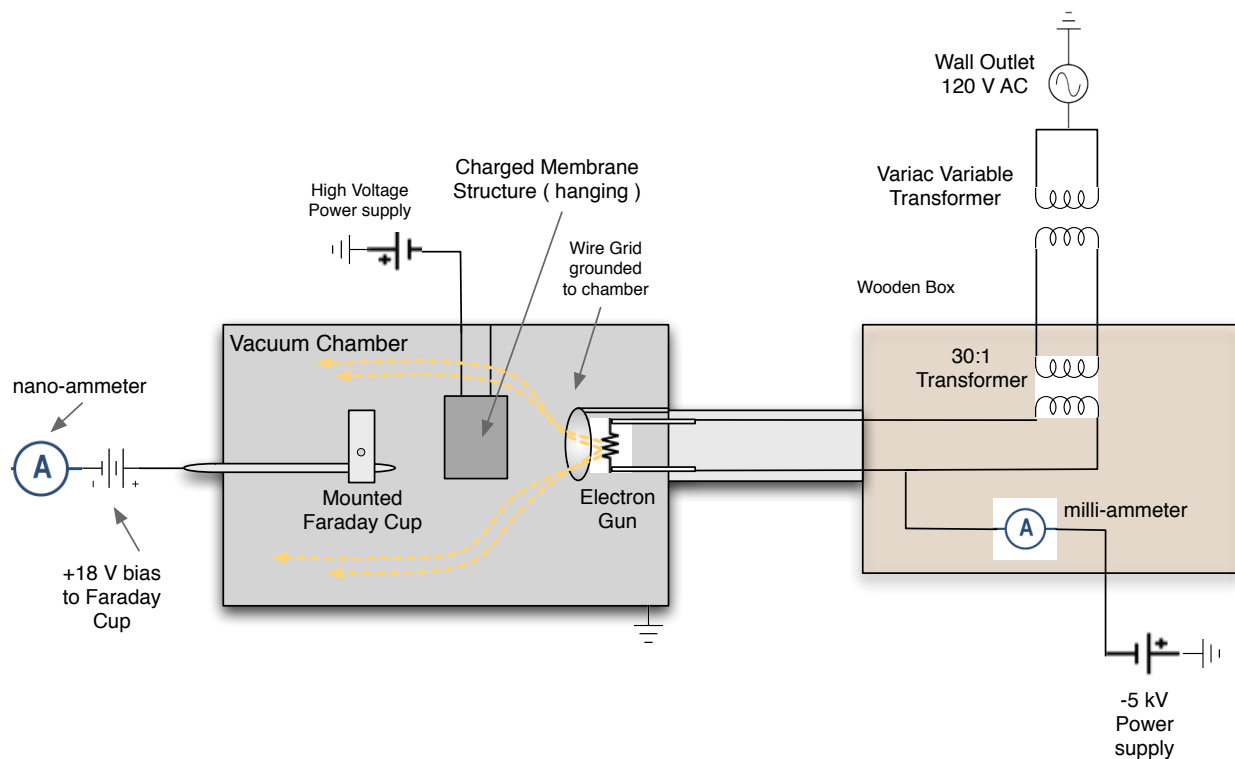


Figure 2.4: Final Radiation experiment hardware setup

erated off by the electrostatic field between the filament and the grounded wire mesh. The filament is constructed of 5mil coiled Tungsten wire. The length of the Tungsten wire was chosen based on the resistivity of the metal, ρ , and the electrical resistance, R . The resistivity of Tungsten near the melting point is approximately 10^{-6} Ohm-meters and the electrical resistance was measured in the lab to be 2-3 Ohms. Using Equation (2.1), the 5 mil wire (cross sectional area, $A = 1.3e^{-8}$) could have a length, l , of approximately 3.8 cm.

$$l = R \frac{A}{\rho} \quad (2.1)$$

The current emitted from the tungsten coil can be tuned by changing the setting of the Variac variable transformer. The higher the AC current supplied to the coil, the higher the temperature, thus more electrons can be accelerated toward the grid. The high voltage power supply providing the DC bias to the coil is current-limited at 5 mA, therefore the maximum emission current is 5 mA.

The FC-70 Faraday cup was chosen as the device to detect current inside the chamber. The detector has a small aperture into which electrons can flow to measure the ambient current. The FC-70, shown in Figure 2.6 is mounted onto an aluminum plate with a collar attached with vacuum epoxy. The collar allows for mounting the device onto a rotatable vacuum feedthrough probe. The rotatable probe allows the Faraday cup to sweep through an angular range of approximately 120° , thus providing positioning both behind and to each side of the membrane structure.

The output of the Faraday cup is connected to a digital multimeter with DC current resolution to picoAmps. A battery is located in the path between the nano-ammeter and the Faraday cup. The battery is a combination of the two 9 Volt batteries connected in series to bias the Faraday

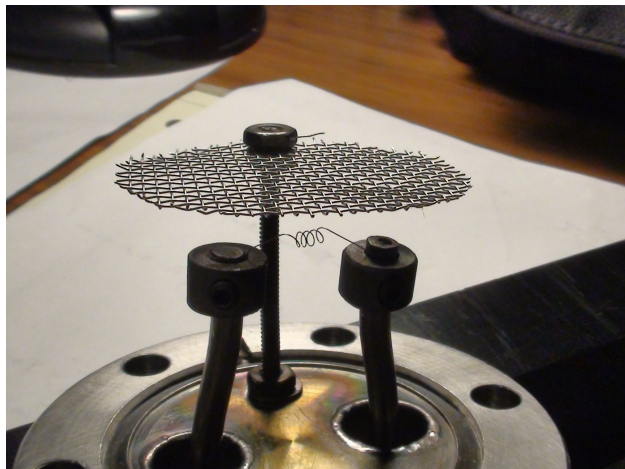


Figure 2.5: *Electron gun filament and wire mesh*

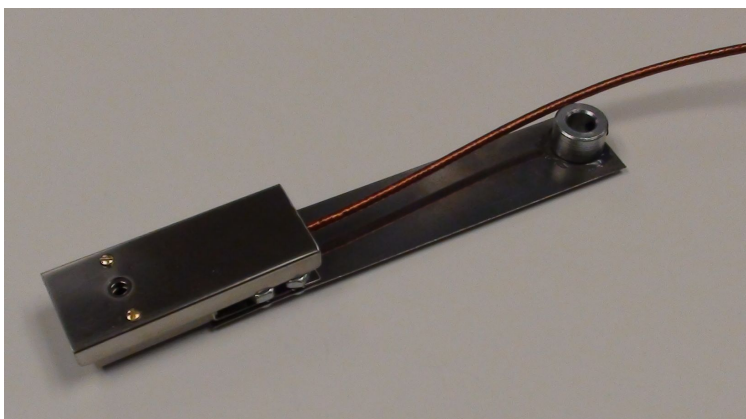


Figure 2.6: *Mounted Faraday cup with collar for attachment to vacuum feedthrough*

cup by 18 V. This small voltage helps to eliminate low-energy secondary electrons from entering the aperture of the Faraday cup.

2.3 Experimental Structures

A range of membrane structures were constructed from Aluminized Mylar for the radiation experiments. Four different configurations were used for the final experiments, including sheets with cutouts, and different orientations of membranes connected with membrane ribs or ties. For a longer duration study, it would be desirable to test a much larger range of structures. The ribbed box-structure was chosen as it was the baseline configuration used to study the EIMS concept in Reference 1. The ribs serve the purpose to limit the separation distance between sheets. As will be later discussed, the rib structure did not inflate fully at the low voltages, therefore the rib function was replaced by wire ties. The ties were less restrictive and allowed for better inflation. The cutout structures were included to study how the electrostatic fields, not including the materials itself, can shield particles. The cutout structure could also offer further mass savings, and the edges of the cut-outs can serve to focus local charge concentrations given a fixed EIMS potential.

Each of the four configurations are briefly described with comments to aid in understanding

the experiments described in the remainder of the report. Illustrations of each configuration are shown in Figure 2.7

Table 2.1: Membrane structure configurations for radiation experiments

Structure Configuration	Comments
A) Two unconnected membranes with rectangular cutouts	Two 8cm x 15cm sheets with 4cm x 7cm rectangular cutout; Membranes inflated in sideways configuration;
B) Two membranes, connected with ribs	8cm x 15cm sheets; Two 1.5cm membrane ribs attached with vacuum rated epoxy;
C) Two membranes, connected with ties, face	8cm x 10cm sheets; Tied at Corners; Large area facing electron gun
D) Two membranes, connected with ties, edge	8cm x 10cm sheets; Tied at Corners; Edges facing electron gun

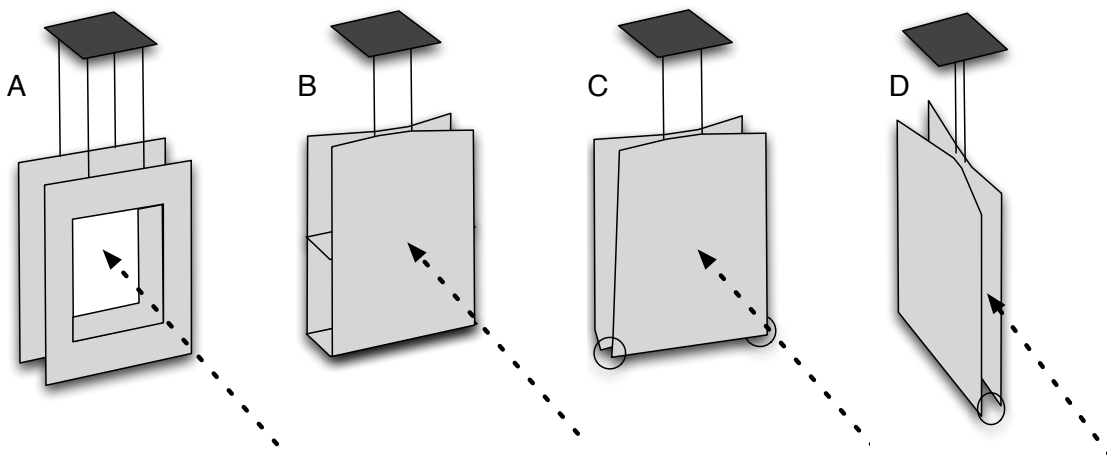


Figure 2.7: Four membrane structure configurations A–D used for experiments. The incoming charge flux direction is shown through the dashed arrow.

Chapter 3

Experiments and Results

3.1 Atmospheric Inflation Experiments

With the high voltage charging setup, tests were conducted to inflate membrane structures in the laboratory environment. Atmospheric inflation experiments allow a quick method to test the capabilities of the high voltage charging system without the rigors of preparing the vacuum system. In particular, this ensures that the EIMS prototypes will be able to inflate in the vacuum setup. The atmospheric conditions are actually more challenging in regard to the inflationary forces created due to the coupling with the atmospheric ionization that occurs with kilo-Volt potentials. First tests included charging of two independently hanging sheets of aluminized Mylar. Figure 3.1 shows the inflation during a test where each sheet was charged to 10 kV.

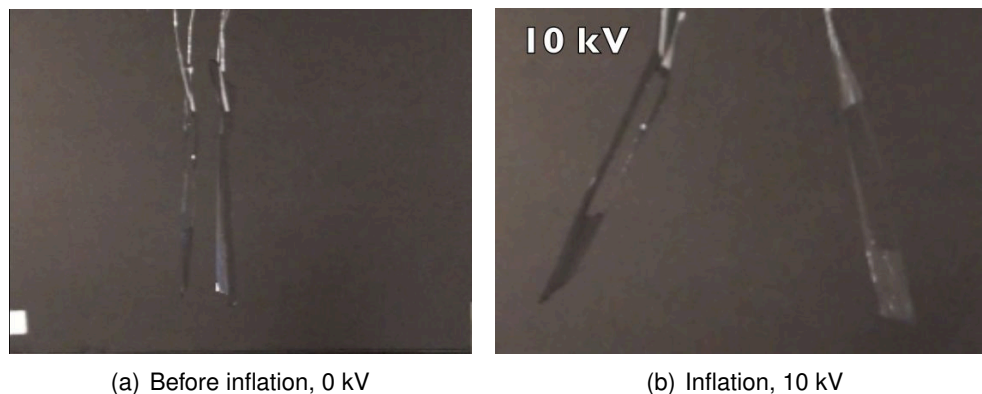


Figure 3.1: *Uncharged and charged hanging membranes during a laboratory inflation test*

Figure 3.2 shows inflation of another membrane structure which was tested in atmospheric conditions. The membranes sheets are cut with a series of slits to study if edge effects at the slits can provide larger electrostatic fields for inflating the membranes. There did not appear to be significant differences between a solid sheet and slitted sheet. What this illustrates is that the EIMS membranes do not need to be solid surfaces. This makes them robust to small tears and ribs from micro-meteorite damages.

For the structures tested in the laboratory, inflation was observed for all EIMS test objects at charging levels as low as 4 kV. Below the 4 kV level, effects from the atmosphere becoming ionized and actually inducing attraction between the membranes was observed. These results



Figure 3.2: *Atmospheric inflation experiment with slitted membrane sheet at 10 kV*

showed that a vacuum environment is critical to simulate how electrostatic inflation may occur in a space-like environment. Because the electron gun only produces energies up to 5keV, it is important that electrostatic inflation is achieved below 5kV. The atmospheric tests illustrated that this is feasible.

3.2 Vacuum Inflation Experiments

During the month of July, the atmospheric inflation test setup was moved to a vacuum chamber. Tests which were conducted in the laboratory were repeated in the approximately 10^{-7} Torr chamber. Previously observed effects in laboratory tests from the atmosphere becoming ionized and inducing attraction between the sheets were not observed in the vacuum chamber, as predicted. It was found that significantly lower voltage magnitudes were required in the vacuum environment to induce the same inflation levels that were seen in the atmosphere at higher voltages. To consider cases where not all electrons are repelled by the structure, it is critical that EIMS are inflated with less than 5kV. The vacuum chamber inflation experiments demonstrate that this is feasible.

Table 3.1 displays information about the inflation experiment results both in atmospheric conditions and in the vacuum chamber.

Figure 3.3 shows several membrane structures tested in atmospheric and vacuum conditions. For all structures tested in the chamber, there is a noticeable transient dynamic response when the potential on the structure is initially changed by several kilovolts without a smooth voltage ramp. This was especially significant for the unconnected structures which would expand beyond their equilibrium inflated position before settling. After the dynamics from inflation settled down, there was no residual movement in the membrane structures. These results can be seen in the video file EDCE-2011-1.mp4.

Table 3.1: Results from key inflation experiments

Experiment	Key Observations and Recommendations
Atmospheric, Rectangular Cutouts	Atmospheric charging setup successful; Need less restrictive mount; Inflation begins near 4 kV; Apparent attraction below 5 kV
Vacuum; Rectangular Cutouts	Vacuum charging setup successful; Tapeless attachment method due to tape adhesive dissolving in sonic bath; Inflation observable at 2 kV and no observable attraction
Atmospheric, Slitted sheet	New mount less restrictive; Some billowing observed around slits; Some mechanical stickage between slits; Inflation begins near 5 kV;
Vacuum, Slitted sheet	Less billowing observed in vacuum; Similar voltage levels required for inflation as rectangular cutout shape, approximately 2.5 kV;
Atmospheric, Tied	Ties functioned to limit separation distance; Need ties which interfere with structure less; Inflation begins near 4 kV;

**Figure 3.3:** Photos of several membrane structures tested in atmospheric and vacuum conditions

Figure 3.4 shows an inflation experiment as seen through a window in the vacuum chamber. Here, the unconnected hanging membranes are charged to 5kV. Without any connecting structures between the two membranes, the sheets inflate in a tapered configuration.

With the current hardware setup, voltage applied to the structure is constrained to a maximum of 5kV. A higher voltage rated vacuum feedthrough will be necessary to charge the structures to the desired level. Currently, inflation can be observed in the 5kV and lower range, but higher voltages would lead to more inflation and more stiffness in the structures. In laboratory conditions, much higher voltages can be applied and with charging to the 20kV range, more pronounced inflation is observed.



Figure 3.4: *Inflation experiment with membranes at 5kV (configuration A) being performed in the vacuum chamber*



Figure 3.5: *Inflation experiment with ribbed structure (Configuration B) at 5kV being performed in the vacuum chamber*

3.3 Charge Deflection Experiments

Two main experiments were performed for each of the four structure configurations. The first, referred to as shielding experiments, studied how the detected current behind a membrane structure changed for different structure voltages and different electron energies. The second experiment, referred to as charge deflection pattern experiments, involved sweeping the angular position of the Faraday cup from behind the structure to the outside of the structure on each side. These are described in more detail below, along with results.

3.3.1 Shielding Experiments

The setup for the shielding experiments includes the electron gun at one end of the vacuum chamber and the Faraday cup positioned directly behind the membrane structure at the opposite end of the chamber. The gun emits electrons and the Faraday cup will measure the detected current, providing insight into how an EIMS structure can be used for radiation shielding.

The first shielding experiments were performed with the unconnected cutout sheets hanging in the vacuum chamber. For a fixed electron energy and emission current, a sweep of voltages on the membrane structure was performed, up to the 5 kV high voltage rating on the vacuum feedthrough. For each structure voltage, the current detected by the Faraday cup was recorded. This procedure was repeated for different electron energies from 1 to 5 keV. There was a clear trend of decreasing current detected behind the membrane structure as the structure voltage was increased. This can be seen in Figure 3.6(a) for the cutout membranes (configuration A), in Figure 3.6(b) for the ribbed structure (configuration B), and in Figures 3.6(c) and 3.6(d) for the two configurations C and D of the tied structure. In these plots, the percent blockage of current detected with a charged structure relative to the current detected with an uncharged membrane is expressed by contours.

From these figures, several conclusions can be made. A clear trend exists of increased shielding with increased structure voltage for the first three configurations, where the pattern is seen for all electron energies and structure configurations. These figures appear to have roughly the same pattern. For the ideal case of having an electron of energy less than 1keV approach the center of a charged membrane of potential 1kV, the electron should be deflected backwards. Thus, in this ideal scenario we should not be measuring charge behind the structure if the EIMS voltage is above the electron energy voltage. However, these tests of similarly sized EIMS prototypes illustrate that this is only approximately the case. The electron beam is not focused, and as a result there is bending of the charge flux about the edges, as well as interactions with the grounded vacuum chamber walls. Differences in the charge deflection amount were observed for different EIMS shapes. For example, the cut-out membrane structure (configuration A) provides only a small loss in charge deflection in contrast to the more solid membrane structures. This indicates that very open charged structures might provide very light-weight charge deflection capabilities.

An interesting deviation from the nominal charge deflection to EIMS voltage relationship is seen in Figure 3.6(d). Here, for the tied configuration with the edge facing the electron gun, the current begins to instead increase at the highest structure voltage. A reason for this can be seen in Figure 3.8. Below a structure voltage of 5 kV, the membranes are physically blocking the Faraday cup aperture. When 5kV is achieved, inflation of the two membranes creates an opening in front of the aperture. As there is theoretically no electrostatic field between two like-charged sheets, the shielding begins to degrade. This illustrates that the complex flexible shape interactions with the resulting electrostatic force field must be carefully considered when designing such active charge deflection systems.

Also note that the contour plot for the unconnected cutout membranes (configuration A) is only shown for structure voltages up to 4kV. At a charging level of 5 kV, the membrane structure inflates until physically touching the wall of the vacuum chamber. Once the membrane contacts the grounded chamber, the structure begins to draw a large current from the high voltage power supply and must be shut down.

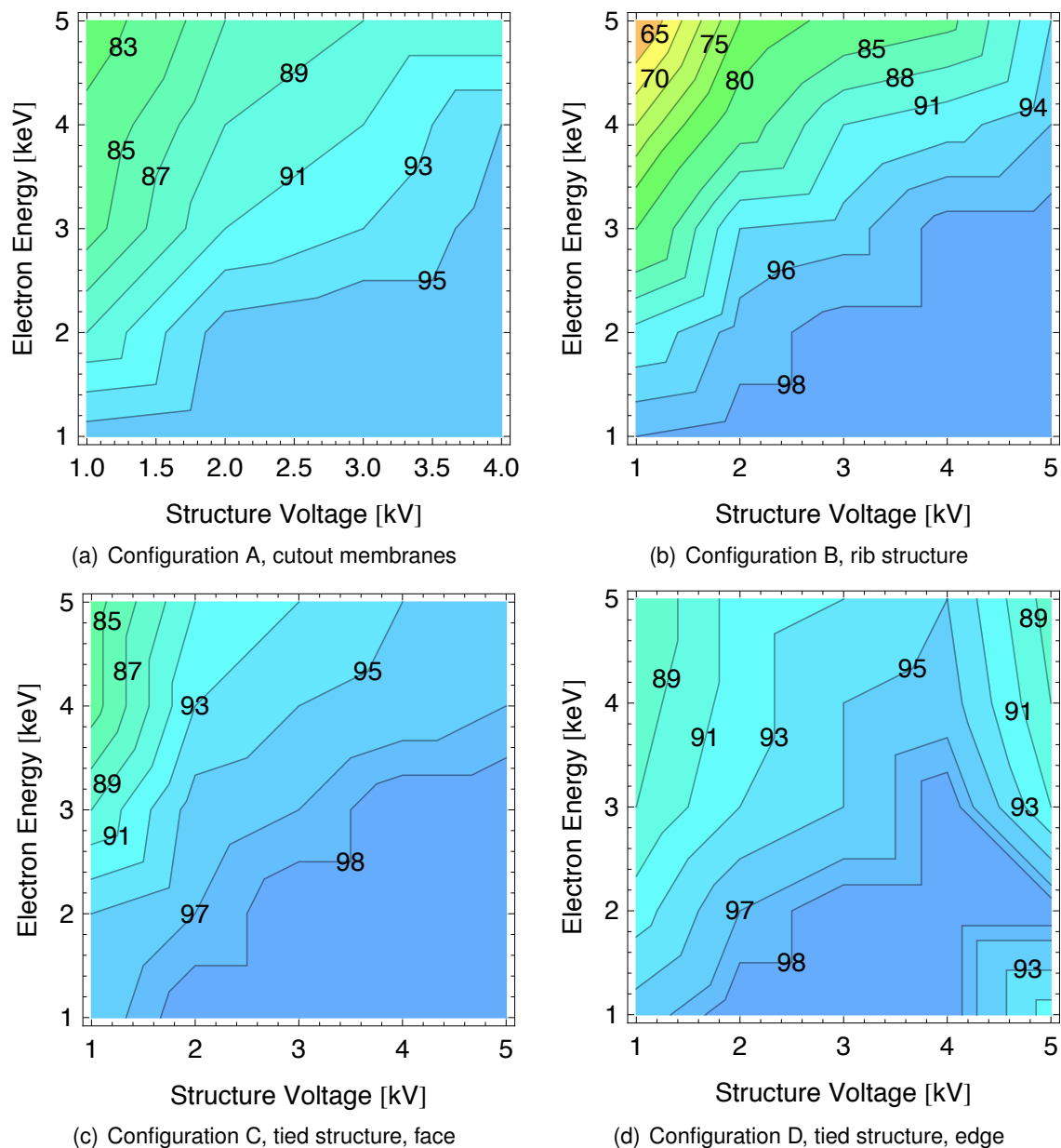


Figure 3.6: Percent blockage of original detected current behind inflated membrane structure at different electron energies

3.3.2 Charge Deflection Pattern

To study the charge deflection and shielding pattern around the membrane structure, the Faraday cup position is rotated within the chamber. The probe on which the detector is mounted allows for rotation through approximately 120 degrees. Measurements of detected current are recorded as the probe and detector are swept through the physically feasible angular range. The rotation of the detector is illustrated in Figure 3.9.

This experiment was performed with each of the four configurations listed in Table 2.1. Plots are included to describe the results of these tests. Figure 3.10 illustrates the difference in pattern

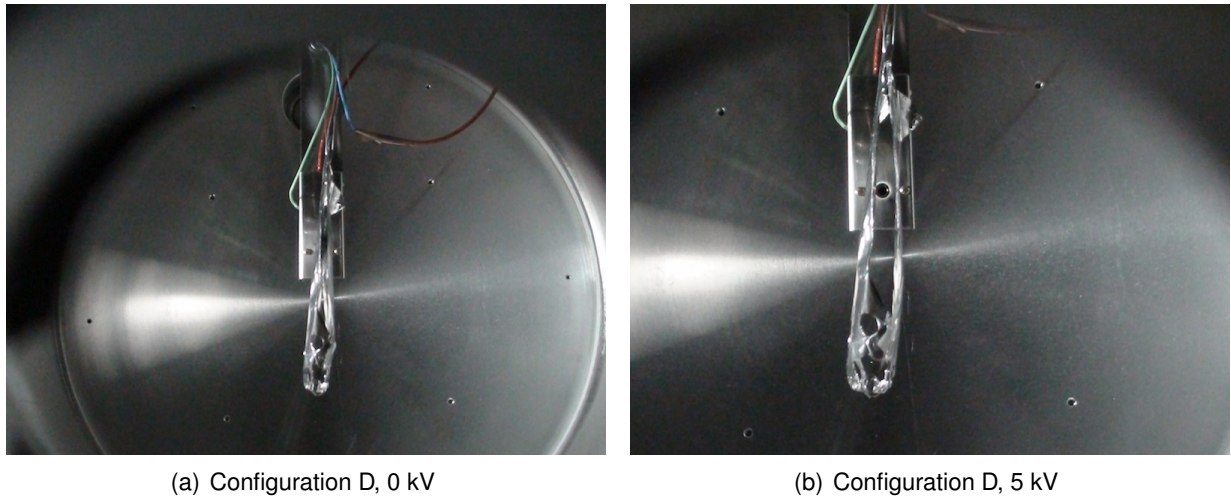


Figure 3.7: *Physical blockage of Faraday cup aperture at 0kV and inflation creating a physical path to aperture at 5 kV*

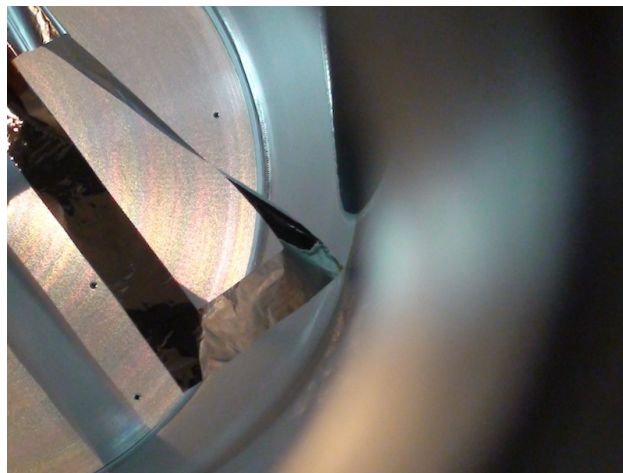


Figure 3.8: *Inflated membrane structure making contact with grounded chamber wall*

of electrons with no membrane structure in the vacuum chamber and a single, charged membrane sheet. The sheet physically blocks the Faraday cup from approximately -10° to $+45^\circ$. There is a clear drop in detected current behind the charged structure and also in the areas surrounding the structure.

Figure 3.11 shows the pattern of detected current behind the double membrane structure connected with ribs with electrons at 2 keV. Three scenarios are displayed: an uncharged structure, a structure charged below the electron energy (1 kV), and a structure charged above the electron energy (3 kV). The results from this figure are clear that the shielding increases with increasing structure voltage. The angular range over which shielding occurs also widens as the voltage is increased on the structure. Until the very extreme angles of the detector position, nearly all electrons are shielded in the 3 kV charging scenario. The results of this test clearly display the radiation shielding capability of a charged structure, especially the double membrane configuration.

Similarly, the plots for the two tied configurations are shown in Figures 3.12 and 3.13. These plots show the same trend as the previous plot for the ribbed structure. One interesting observation

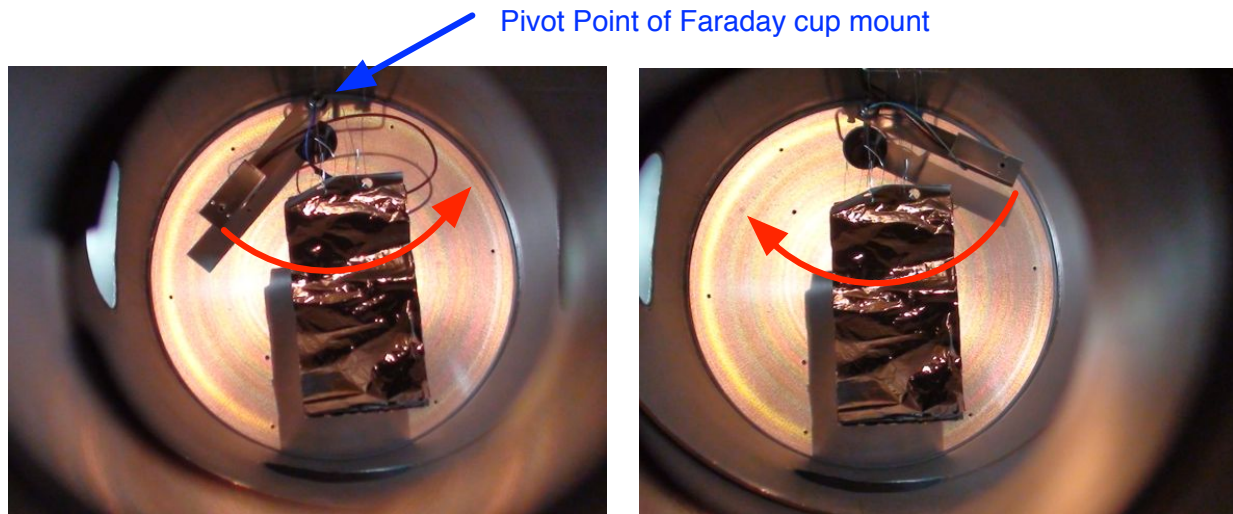


Figure 3.9: Rotation of the Faraday cup around the membrane structure

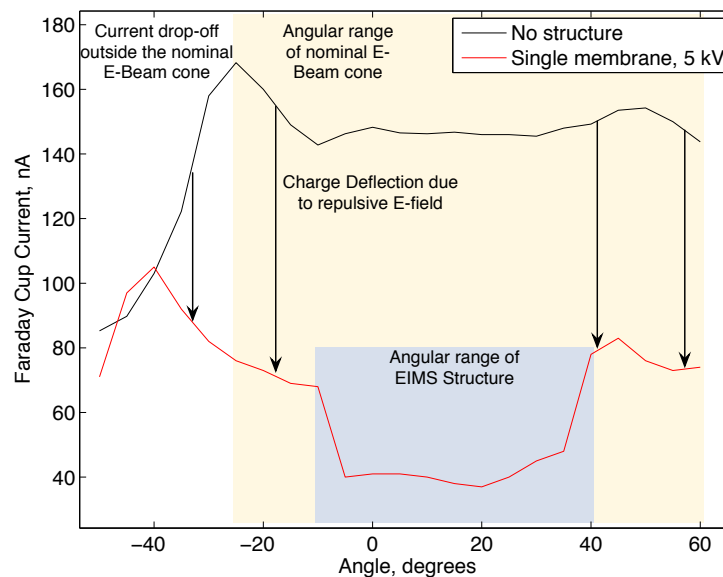


Figure 3.10: Detected electron pattern for Faraday cup angular sweep with no membrane structure versus a charged single-membrane structure

is the clear difference in the current readings behind the uncharged membrane for the two tied configurations. When the large area of the structure is facing the electron gun, there is a large dip corresponding to the physical dimension of the sheet. For the edge configuration, a very small dip is seen, as the Faraday cup is only physically behind the structure through a few degrees of the sweep. This shows how the structure is also passively acting as a radiation shield.

3.3.3 Stability in an Electron Flow

The stability of the membrane structure in the electron flow was studied, particularly with the unconnected membrane sheets. When the electron gun is emitting and the structure is charged, there are visible vibrations of the sheets. In general, vibrations increase in both amplitude and

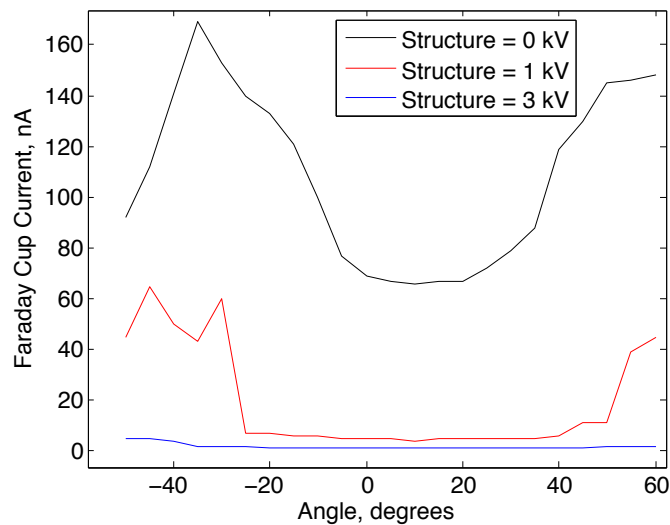


Figure 3.11: Detected electron pattern for Faraday cup angular sweep with membrane structure at different voltages; Configuration B

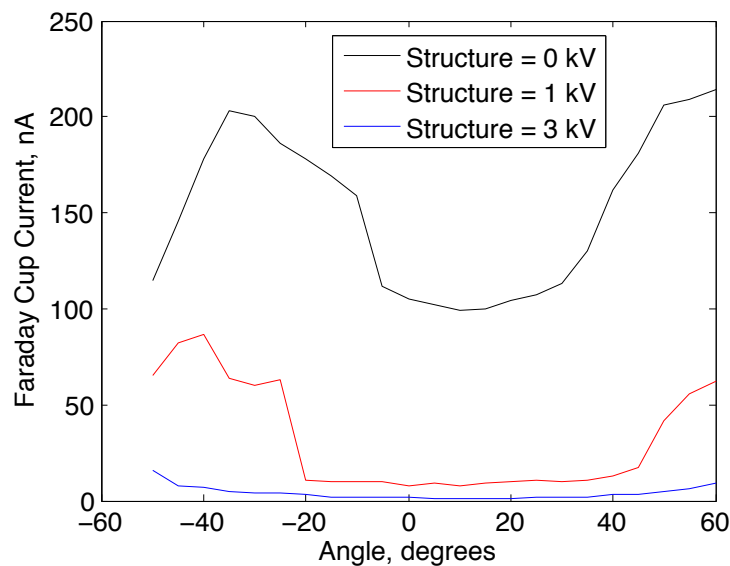


Figure 3.12: Detected electron pattern for Faraday cup angular sweep with membrane structure at different voltages; Configuration C

frequency as the structure voltage is raised. The vibrations also increase while the current from the electron gun is increased. The highest frequency vibrations were observed at the upper limit of the structure voltage (5 kV), electron energy (5 keV) and emitted current (5 mA). An exception to this trend was observed for extremely small currents (approximately 0.03 mA) with a charged structure. Vibrations were observed in a range of just a few fractions of milliAmps then seemed to disappear. Further investigating this effect is future work.

Figure 3.14 is shown to convey the magnitude of vibrations in the structure. It is difficult to capture the small oscillations, but a difference can be seen in the membrane shadows of Figure 3.14.

It was also observed that having the electron flow present when increasing the structure voltage

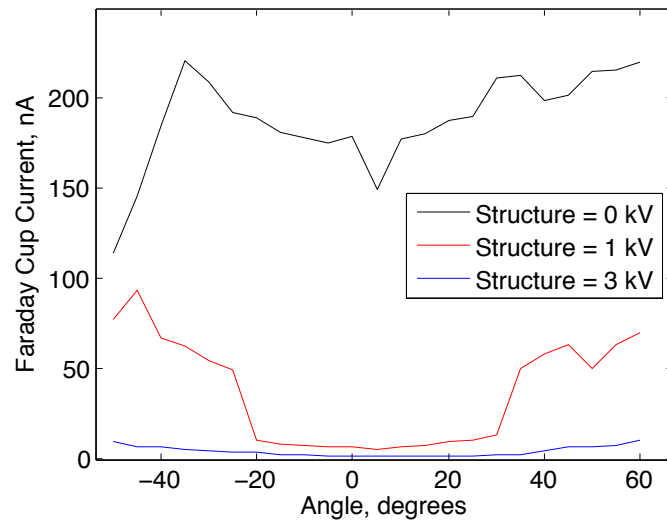
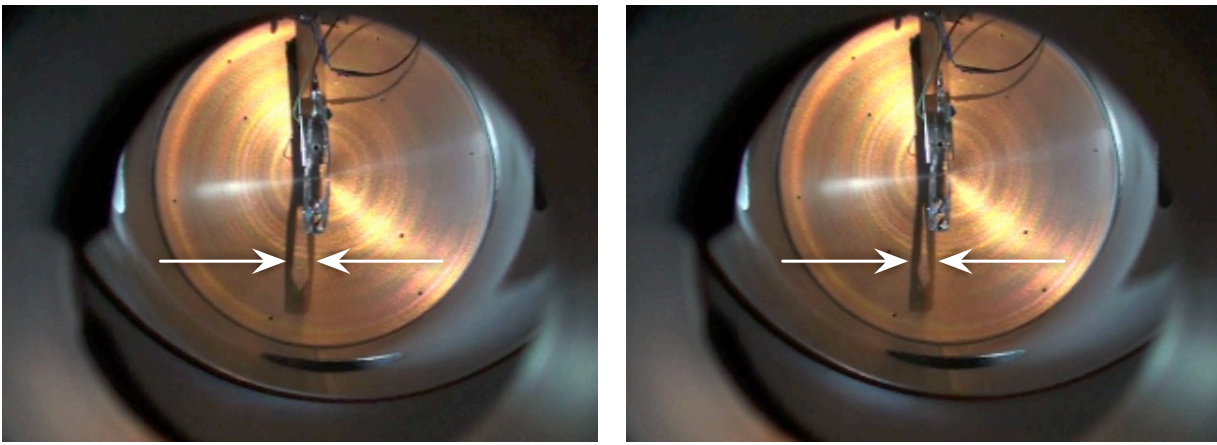


Figure 3.13: Detected electron pattern for Faraday cup angular sweep with membrane structure at different voltages; Configuration D



(a) Slightly expanded position during vibration

(b) Slightly deflated position during vibration

Figure 3.14: Video snapshots to illustrate magnitude of structural oscillation; As shown by arrows, difference enhanced in shadow

can amplify the inflation movement and reduce the damping of this movement. It is recommended to use small increases in voltage to avoid the amplified behavior from a large jump in structure voltage. Video captured of the vibrations can be seen in the video file EDCE-2011-2.mp4.

Chapter 4

Conclusions and Future Work

4.1 Study Conclusions

In this study, it was shown that radiation shielding for low energy (1 - 5 keV) electrons can be achieved by active shielding with an electrostatically inflated membrane structure using similar potential energy levels. In general, higher voltages on the membrane structures lead to improved radiation shielding and charge deflection. Open membrane concepts with holes or slots yield similar charge deflection performance as the solid structures. This illustrates the robustness of such concepts to small local damages due to micro-meteorites. Further, a non-solid membrane concept will enable further mass savings. Plots are presented to describe both the shielding capabilities and the charge deflection patterns for several different membrane structures. At high structure voltages and electron energies, small oscillations are observed in the membrane structure, but the structures do not become unstable. Many of the results will be further investigated as part of future work.

4.2 Future Work Considerations

There are several improvements which could be made to the current setup to refine the results. First, the current electron gun setup accelerates electrons into a wide spray pattern. If the gun could accelerate electrons in a more direct line, a better understanding of the radiation shielding could be gained without the undesirable wide angle spray. The spray pattern modification could be made by adding deflection plates to the gun setup. Also advantageous would be a larger vacuum chamber. A larger chamber would reduce the boundary effect of the grounded chamber being within approximately ten centimeters of the membrane structure. There were occasionally inflations in which the structure actually touched the grounded chamber wall, as shown in Figure 3.8. This was an issue for the power supply as the current drawn became very large. Also, a vacuum feedthrough with a higher voltage rating is desirable to allow higher structure voltages. Inflation is currently limited by this 5kV maximum applied voltage.

Additionally, a better understanding of the physical processes inside the chamber need to be better understood. This will be achieved by an analytical study of the physical phenomena and also through numerical simulation of the chamber environment.

Bibliography

- [1] Stiles, L. A., Schaub, H., Maute, K. K., and Daniel F. Moorer, J., “Electrostatic Inflation of Membrane Space Structures,” AAS/AIAA Astrodynamics Specialist Conference, Toronto, Canada, Aug. 2010.
- [2] Stiles, L. A., Schaub, H., and Maute, K. K., “Voltage Requirements for Electrostatic Inflation of Gossamer Space Structures,” AIAA Gossamer Systems Forum, Denver, Colorado, Apr. 2011.
- [3] Bittencourt, J. A., *Fundamentals of Plasma Physics*, Springer, 3rd ed., 2004.
- [4] Spillantini, P., Casolino, M., Durante, M., Mueller-Mellin, R., Reitz, G., Rossi, L., Shurshakov, V., and Sorbi, M., “Shielding from cosmic radiation for interplanetary missions: Active and passive methods,” *Radiation Measurements*, Vol. 42, No. 1, 2007, pp. 14 – 23.
- [5] Townsend, L. W., “Overview of active methods for shielding spacecraft from energetic space radiation,” *Physica Medica*, Vol. 17, 2001, pp. 84–85.
- [6] Tripathi, R. K., Wilson, J. W., and Youngquist, R. C., “Electrostatic Space Radiation Shielding,” *Advances in Space Research*, Vol. 42, No. 42, 2008, pp. 1043–1049.